Electronic Supplementary Material (ESI) for Chemical Communications.

Suppporting information
ChemComm

Conjugated Polymer Donor-Molecular Acceptor Nanohybrids for Photocatalytic Hydrogen Evolution

Haofan Yang, Xiaobo Li,* Reiner Sebastian Sprick and Andrew I. Cooper*

Table of Contents

Experimental Procedures

1.1 Materials

Poly[*N*-9'-heptadecanyl-2,7-carbazole-*alt*-5,5-(4',7'-di-2-thienyl-2',1',3'-benzothiadiazole)] (D1), poly(9,9-di-*n*-octylfluorene-*alt*-bithiophene), poly[(9,9-di-*n*-octylfluorenyl-2,7-diyl)-*co*-bithiophene] (D2), poly(9,9-di-*n*-octylfluorene-*alt*-benzothiadiazole) (D3), poly[2-methoxy-5-(2-ethylhexyloxy)-1,4-phenylenevinylene] (D4), poly(3-hexylthiophene-2,5-diyl) (D5), [6,6]-phenyl-C61-butyric acid methyl ester (A1), [6,6]-phenyl-C71-butyric acid methyl ester (A2), indene-C60-propionic acid butyl ester (A3) and 3,9-bis(2-methylene-((3-(1,1-dicyanomethylene)-6,7-difluoro)-indanone))-5,5,11,11-tetrakis(4-hexylphenyl)-dithieno[2,3-*d*:2',3'-*d*']-s-indaceno[1,2-*b*:5,6-*b*']dithiophene (A4) were obtained from Ossila (U.K). Poly(sodium 4-styrenesulfonate), poly(styrene-*alt*-maleic acid) sodium salt solution, sodium dodecyl sulfate (SDS), ascorbic acid (AA), hexachloroplatinic acid solution (8 wt. % in water) and tetrahydrofuran (THF inhibitor-free) were purchased from Sigma-Aldrich. Metal precursors were obtained from commercial suppliers Sigma-Aldrich, TCI and Alfa Aesar. The deionized water was purified using a Milli-Q System (ρ = 15 MΩ). All chemicals were used as received without further purification.

1.2 Synthesis of DANHs

The donor and acceptor materials were dissolved in anhydrous THF with a concentration of 0.2 mg mL^{-1} and 1 mg mL^{-1},[1] respectively, serving as stock solution. A volume of 1 mL of the donor and the acceptor stock solutions was mixed together and sonicated for a few minutes. Next, 0.5 mL of this mixture was added rapidly into a vial containing 5 mL of deionized water under continuous sonication for around 10 seconds. All samples were placed in a cover-free sample holder on a hot plate at 130 °C for 5 hours to completely evaporate the residual THF. For the preparation of pure donor or acceptor nanomaterials, all procedures were the same except that 1 mL of donor or acceptor stock solution was used.

1.3 Characterization methods

SEM Measurements were carried out on Hitachi S-4800 cold field emission scanning electron microscope (FE-SEM). Images were collected at working voltage of 10 kV and a working distance of 3.4 mm using a combination of upper and lower secondary electron detectors. Samples were dropped on silica wafer before imaging. ^{1}H NMR spectra were recorded at 400 MHz using a Bruker Advance 400 NMR spectrometer. The UV-visible absorption spectra and steady-state photoluminescence spectra were measured on a Shimadzu UV-2550 UV-Vis spectrometer and an Edinburgh Instruments LS980-D2S2-STM spectrometer, respectively. Samples with good aqueous dispersibility were synthesized by a moderate evaporation method (heating overnight at 60 °C with stirring) and diluted with an appropriate amount of water to keep the sample concentration at 0.01 mg mL^{-1} before measuring the spectrum.

1.4 High throughput photocatalysis measurement

Before photocatalysis, certain amounts of 1 M ascorbic acid solution and hexachloroplatinic acid solution were added into vial (volume = 12 ml) containing 5 ml of above prepared DANHs aqueous solution. The photocatalytic H_2 production activities were then evaluated using a high-throughput degas-irradiation-analysis system. Specifically, after purging with nitrogen for 3 hours in a Sweigher robot (Chemspeed Technologies), the vials were capped with pierceable caps using a capper tool a nitrogen atmosphere. Next, up to 48 vials were illuminated using a solar simulator (A4.5G, Class AAA, IEC/JIS/ASTM, 1440 W xenon, 12 × 12 in., MODEL:94123A) for 2 hours. The samples were rotated and rocked on their sides during irradiation. Gaseous products were injected via a transfer line equipped with headspace injector and the H_2 production was analyzed using an Shimadzu HS-GC.

1.5 Hydrogen evolution kinetics experiments

Kinetic measurements were conducted in a 69 mL quartz flask. Catalysts (normally 1.15 mg for A1/D1) were dispersed into 0.1 M ascorbic acid water solution (25 mL) with diluted hexachloroplatinic acid solution as a platinum precursor (3% to 9% loading). After bubbling with N_2 for 30 min to remove O_2, the reaction mixture was illuminated with a 300 W Newport Xe light-source (Model: 6258, Ozone free) using a 420 nm cut-off filter. The light source was cooled by water circulating through a metal jacket. Gas samples were taken out by using a gas-tight syringe and run on a Bruker 450-GC gas chromatograph. Hydrogen was detected with a thermal conductivity S3 detector referencing against standard gas with a known concentration of hydrogen. Any hydrogen dissolved in the reaction mixture was not measured and the pressure increase generated by the evolved hydrogen was neglected in the calculations. After the photocatalysis experiment, samples were recovered by washing with water and centrifuging twice at 14000 rpm for 15 min. For calculations of the initial hydrogen evolution rate for A1/D1, the first hour of activity was not counted because of the induction time needed for Pt co-catalyst photodeposition to occur.

1.6 Apparent quantum yield measurements

The apparent quantum yield for the photocatalytic H_2 evolution was measured using a λ = 420 nm LED (129.5 mW), λ = 490 nm LED (97.1 mW), λ = 515 nm LED (65.7 mW) and λ = 595 nm LED (115.0 mW) controlled by an IsoTech IPS303DD power supply. For the measurement, 6 vials of A1/D1 sample, prepared by nano-precipitation strategy, were mixed together and then diluted to 25 mL with deionized water. Then, 440 mg of ascorbic acid (0.1 M) and diluted hexachloroplatinic acid (9% loading) were added before illuminating with LED. The light intensity was measured with a ThorLabs S120VC photodiode power sensor controlled by a ThorLabs PM100D Power and Energy Meter Console and the apparent quantum yield was estimated using the equation below:

$$AQY = 2 \times \frac{moles\ of\ hygrogen\ evolved}{moles\ of\ incidentphotons} \times 100\%$$

Supporting Figures

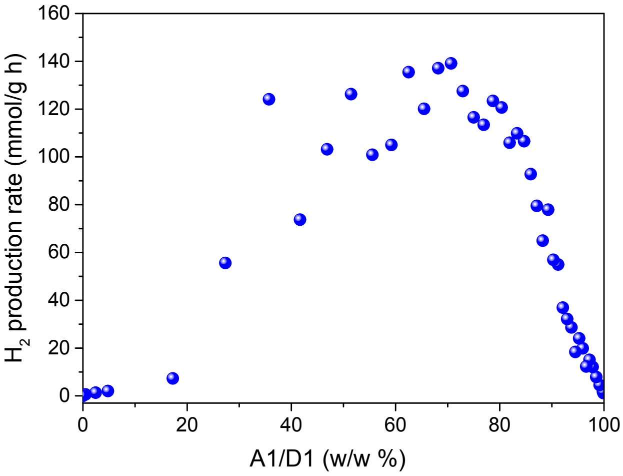

Fig. S1. Photocatalytic hydrogen production rate for A1/D1 NADHs as a function of A1 fraction. Conditions: Catalyst concentration: 20–100 μg mL^{-1} (0.1-0.5 mg in 5 mL water); ascorbic acid: 0.04 M; Pt loading: 3% wt. % (using H_2PtCl_6 8 wt. % in water); light source: solar simulator, 1 sun; irradiation time: 2 hours.

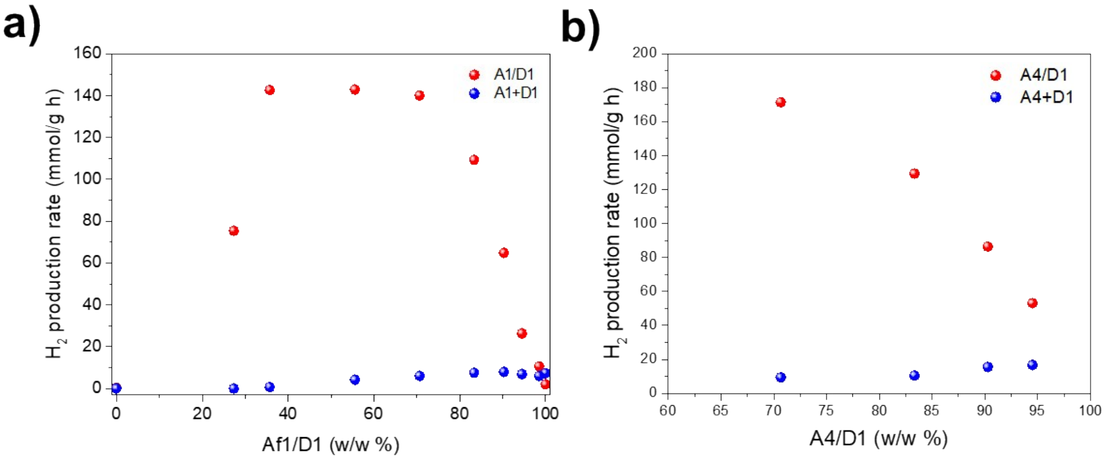

Fig. S2. H_2 production rate of A1/D1 and A1+D1 as a function of A1 fraction. Conditions: catalysts concentration: 20–100 μg mL^{-1} (0.1-0.5 mg in 5 mL water); ascorbic acid: 0.04 M; Pt loading: 3 wt. % (using H_2PtCl_6 8 wt. % in water); light source: solar simulator; irradiation time: 2 hours.

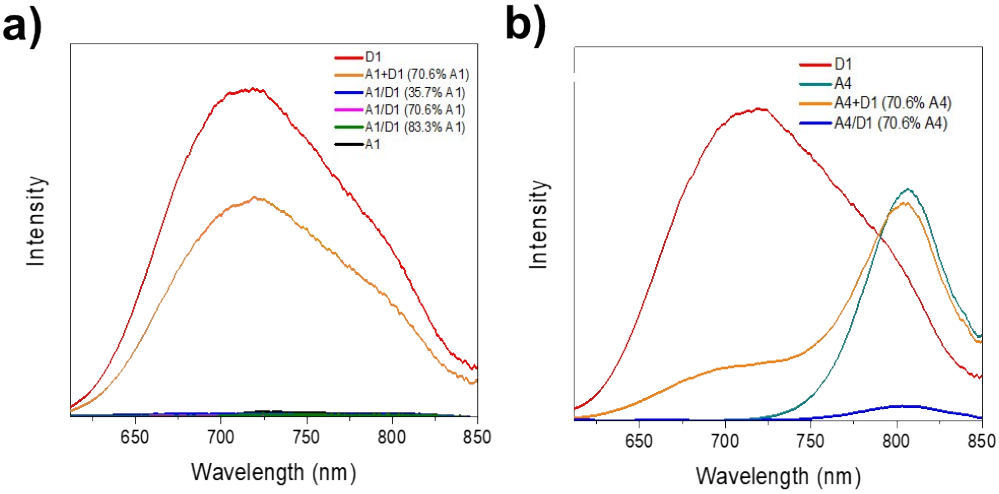

Fig. S3. Emission spectrum of (a) A1/D1 NADHs under 375 nm excitation and (b) A4/D1 NADHs under 600 nm excitation, compared with their physical mixture counterparts (A1+D1 and A4+D1). Measurements were carried out at ambient temperature in aqueous solution.

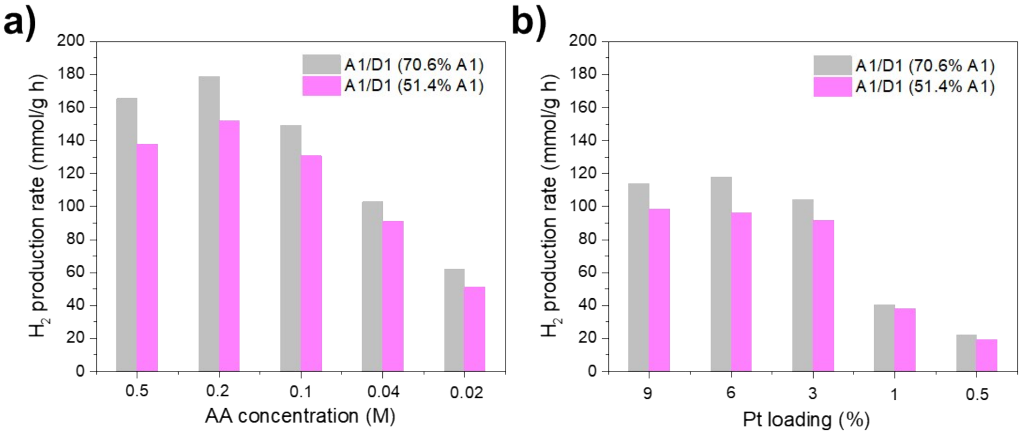

Fig. S4. (a) Effect of ascorbic acid concentration on H_2 production rate under solar simulator irradiation. Catalyst concentration: 46 or 34 µg mL^{-1} (0.23 or 0.17 mg in 5 mL water); ascorbic acid: 0.02–0.5 M; Pt loading: 3 wt. % (using H_2PtCl_6 8 wt. % in water); light source: solar simulator; irradiation time: 2 hours. (b) Amount of Pt loading effect on H_2 production rate under solar simulator. Catalyst concentration: 46 or 34 µg mL^{-1} (0.23 or 0.17mg in 5 mL water); ascorbic acid: 0.04 M; Pt loading: 0.5%–9% (using H_2PtCl_6 8 wt. % in water); light source: solar simulator; irradiation time: 2 hours.

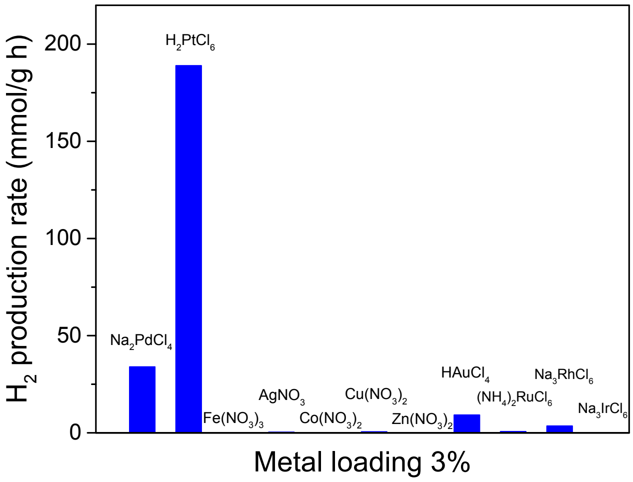

Fig. S5. H_2 production rate for A1/D1 NADHs using various metal precursors. Catalyst concentration: 46 µg mL^{-1} (0.23 in 5 mL water); ascorbic acid: 0.04 M; metal loading: 3 wt. %; light source: solar simulator; irradiation time: 2 hours.

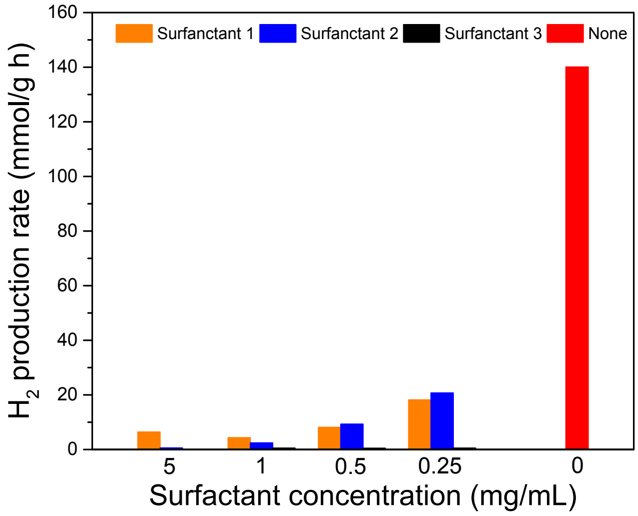

Fig. S6. Effect of surfactants with different concentration on the H_2 production rate for A1/D1 (70.6% A1). Conditions: catalysts concentration: 46 µg mL^{-1} (0.23 in 5 mL water); ascorbic acid: 0.04 M; Pt loading: 3 wt. %; light source: solar simulator; irradiation time: 2 hours. Surfactant 1: SDS, surfactant 2: Poly(sodium 4-styrenesulfonate) and surfactant 3: Poly(styrene-*alt*-maleic acid) sodium salt solution.

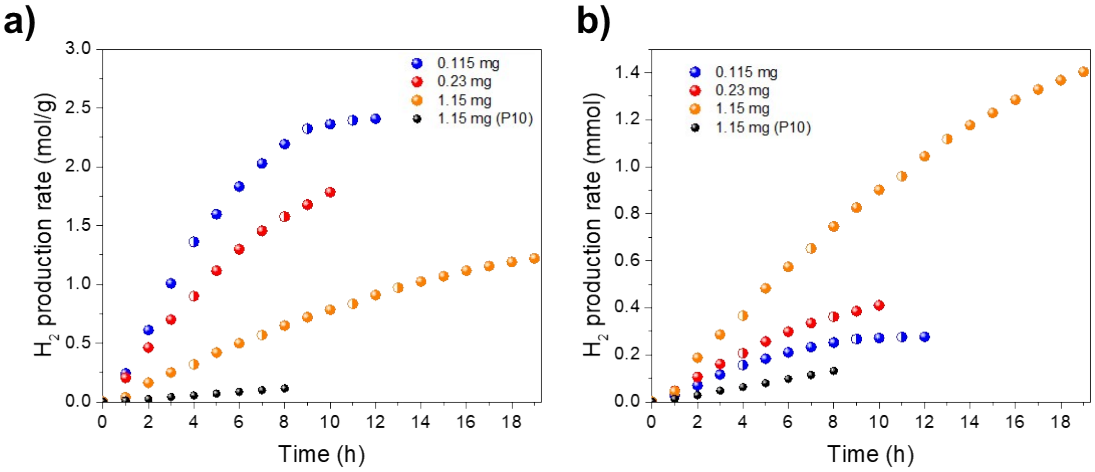

Fig. S7. Time course of (a) mass-normalized and (b) non mass-normalized H_2 production of A1/D1 NADHs. Conditions: ascorbic acid: 0.1 M; Pt loading: 9 wt. % Pt; light source: 300 W Xe light source fitted with a λ > 420 nm filter. Half circle points represent the beginning of next measurement after degassing.

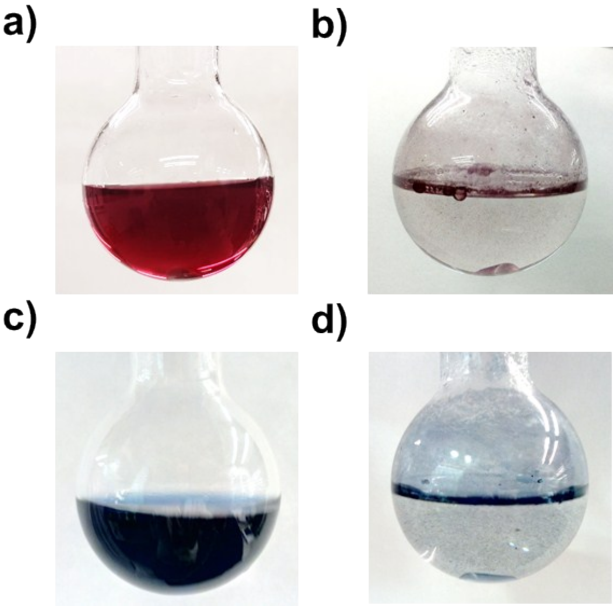

Fig. S8. Image of aqueous A1/D1 reaction solution in a 69 mL flask (a) before and (b) after the photocatalysis experiment (19 hours irradiation). Also, aqueous A4/D1 reaction solution (a) before and (b) after photocatalysis experiment (10 hours irradiation).

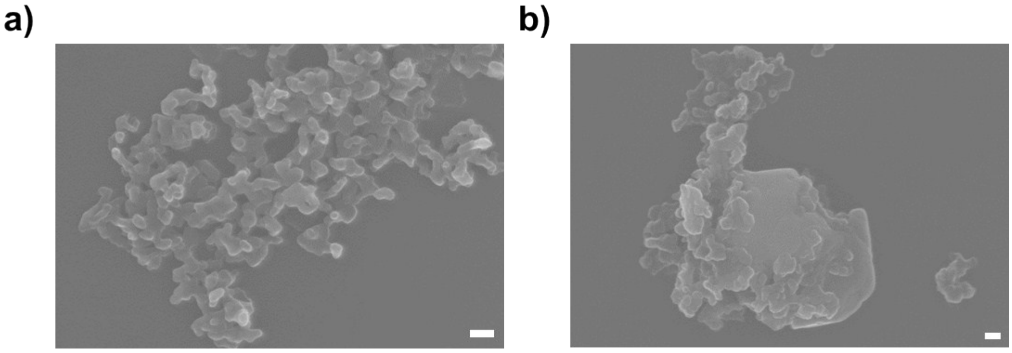

Fig. S9. SEM images of A1/D1 (a) before and (b) after the photocatalysis experiment (scale bar: 100 nm).

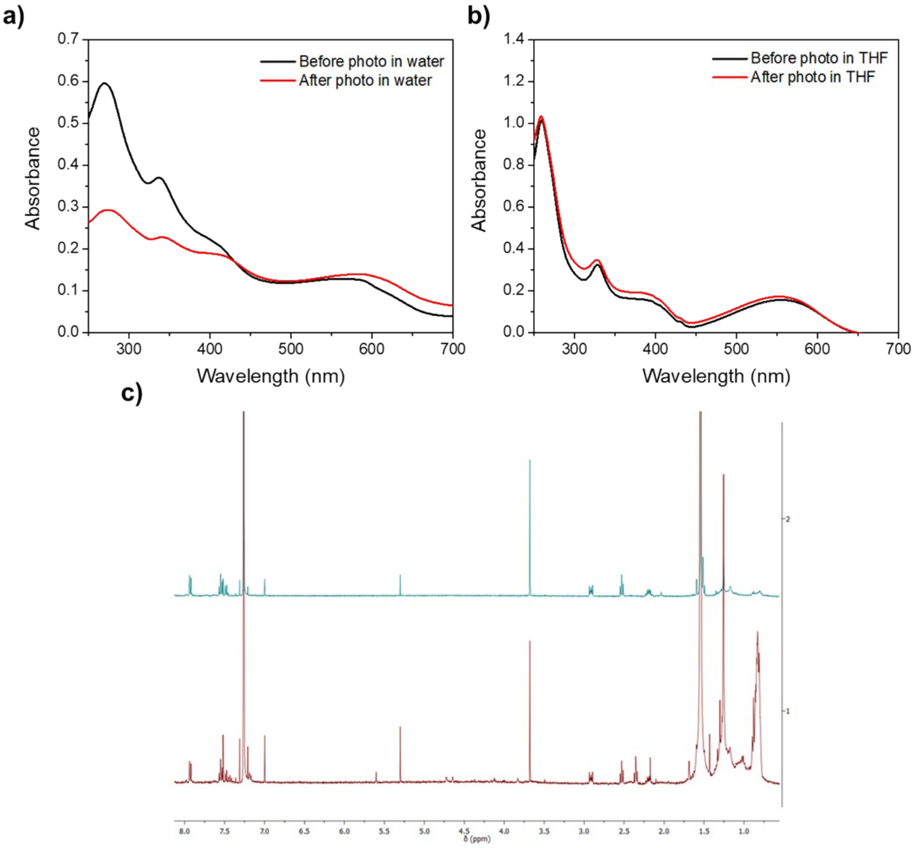

Fig. S10. Absorption spectrum of A1/D1 before and after photocatalysis experiment (a) in water and (b) in THF. (c) ^{1}H NMR of A1/D1 before (top) and after (down) photocatalysis experiment.

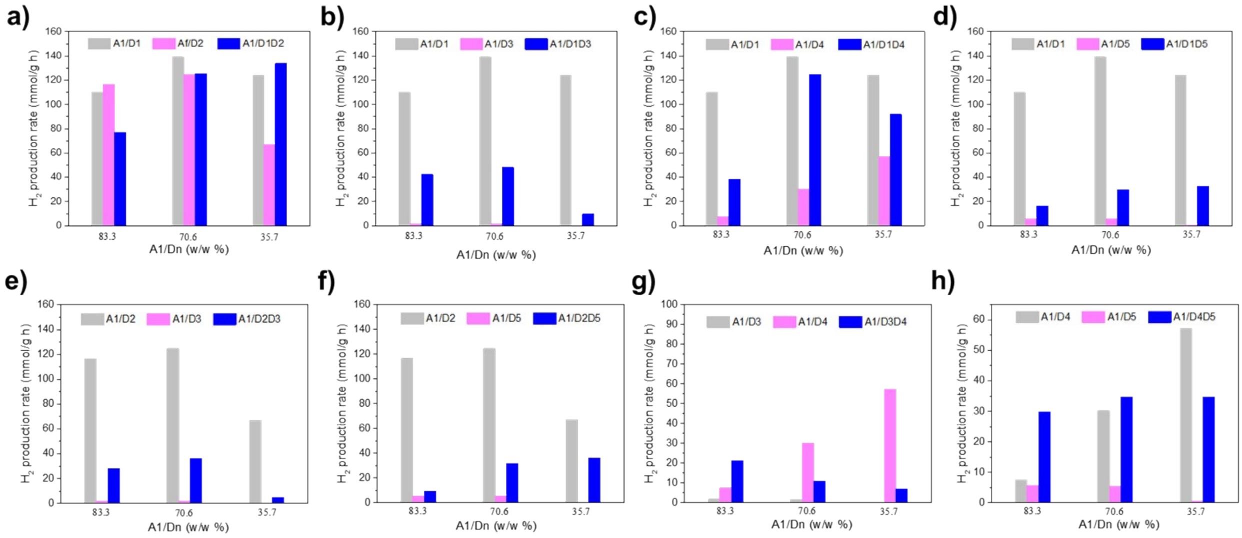

Fig. S11. Hydrogen production rates for various ternary systems with different compositions. Catalyst concentration: 60, 46 and 28 µg mL^{-1} in 5 mL water; ascorbic acid: 0.04 M; Pt loading: 3 wt. %; light source: solar simulator; irradiation time: 2 hours.

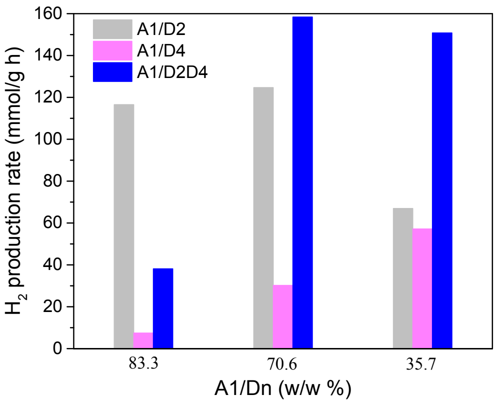

Fig. S12. H_2 production rate for A1/D2D4 ternary NADH system. Conditions: catalysts concentration: 60, 46 and 28 μg mL^{-1} in 5 mL water; ascorbic acid: 0.04 M; Pt loading: 3 wt. %; light source: solar simulator; irradiation time: 2 hours.

Suppporting information
ChemComm

Supporting Table

Table S1. Photocatalytic performance of various reported organic photocatalysts. Note that the HER (and AQY) depends on the irradiation source and experimental set-up, and hence these values can only be comparted in a qualitative sense.

Materials	HER (mmol g^{-1} h^{-1})	AQY	Journal and publication year	Reference
DBTD-CMP_1	9.2 (λ > 420 nm)	0.2% (500 nm)	*ACS Catal.* 2018	[2]
FS-COF FS-COF+dye	10.1 (λ >420 nm) 16.3 (λ >420 nm)	0.6% (600 nm) 2.2% (600 nm)	*Nat. Chem.* 2018	[3]
g-$C_{40}N_3$-COF	4.1 (λ >420 nm)	3.2% (520 nm) 0.29% (578 nm)	*Nat. Commun.* 2019	[4]
Polymer dots PIFDTBT/g-C_3N_4	0.58 (λ >400 nm)	~0.5% (500 nm) ~0.5% (600 nm)	*Appl. Catal. B Environ.* 2019	[5]
CTF-BT/Th	6.6 (λ >420 nm)	~2.5% (500 nm) N/A (550 nm)	*Angew. Chem. Int. Ed.* 2019	[6]
DA-HM	4.14 (λ >420 nm)	~2% (500 nm)	*Angew. Chem. Int. Ed.* 2018	[7]
g-C_3N_4-MF_{100}	3.6 (λ >420 nm)	~4% (500 nm) ~2% (550 nm)	*Nano Energy* 2019	[8]
P3/CN	13 (λ = 420~780 nm)	~15.8% (550 nm) ~1.5% (630 nm)	*Adv. Funct. Mater.* 2018	[9]
Polymer dots PFTFQ-PtPy15	12.7 (λ >420 nm)	0.4% (515 nm)	*ACS Catal.* 2018	[10]
Polymer dots PFODTBT	63 (λ >420 nm)	0.6% (550 nm)	*Energy Environ. Sci.* 2017	[11]
Pt-PVP-Tp-COF	8.4 (λ >420 nm)	0.6% (475 nm)	*Angew. Chem. Int. Ed.* 2019	[12]
Polymer dots P8T2/g-C_3N_4	0.93 (λ >400 nm)	0.8% (550 nm)	*J. Mater. Chem. A* 2019	[13]
P10	3.2 (λ >420 nm)	11.6% (420 nm) N/A (595 nm)	*Nat. Commun.* 2018	[14]
Ter-CTF-0.7	19.3 (λ >420 nm)	14.78% (550 nm)	*ACS Catal.* 2019	[15]
This work A1/D1 DANHs	105.2 (λ >420 nm)	3.16% (515 nm) 3.02% (595 nm)		

References

[1] T. Ameri, J. Min, N. Li, F. Machui, D. Baran, M. Forster, K. J. Schottler, D. Dolfen, U. Scherf, C. J. Brabec, *Adv. Energy Mater.* **2012**, *2*, 1198–1202.

[2] Z. Wang, X. Yang, T. Yang, Y. Zhao, F. Wang, Y. Chen, J. H. Zeng, C. Yan, F. Huang, J. X. Jiang, *ACS Catal.* **2018**, *8*, 8590–8596.

[3] X. Wang, L. Chen, S. Y. Chong, M. A. Little, Y. Wu, W. H. Zhu, R. Clowes, Y. Yan, M. A. Zwijnenburg, R. S. Sprick, et al., *Nat. Chem.* **2018**, *10*, 1180–1189.

[4] S. Bi, C. Yang, W. Zhang, J. Xu, L. Liu, D. Wu, X. Wang, Y. Han, Q. Liang, F. Zhang, *Nat. Commun.* **2019**, *10*, 1–10.

[5] W. Zhou, T. Jia, D. Zhang, Z. Zheng, W. Hong, X. Chen, *Appl. Catal. B Environ.* **2019**, *259*, 118067.

[6] W. Huang, Q. He, Y. Hu, Y. Li, *Angew. Chemie - Int. Ed.* **2019**, *58*, 8676–8680.

[7] H. Ou, X. Chen, L. Lin, Y. Fang, X. Wang, *Angew. Chemie - Int. Ed.* **2018**, *57*, 8729–8733.

[8] H. Che, C. Liu, G. Che, G. Liao, H. Dong, C. Li, N. Song, C. Li, *Nano Energy* **2019**, 104273.

[9] F. Yu, Z. Wang, S. Zhang, H. Ye, K. Kong, X. Gong, J. Hua, H. Tian, *Adv. Funct. Mater.* **2018**, *28*, 1–13.

[10] P. J. Tseng, C. L. Chang, Y. H. Chan, L. Y. Ting, P. Y. Chen, C. H. Liao, M. L. Tsai, H. H. Chou, *ACS Catal.* **2018**, *8*, 7766–7772.

[11] P. B. Pati, G. Damas, L. Tian, D. L. A. Fernandes, L. Zhang, I. B. Pehlivan, T. Edvinsson, C. M. Araujo, H. Tian, *Energy Environ. Sci.* **2017**, *10*, 1372–1376.

[12] J. Ming, A. Liu, J. Zhao, P. Zhang, H. Huang, H. Lin, Z. Xu, X. Zhang, X. Wang, J. Hofkens, et al., *Angew. Chemie - Int. Ed.* **2019**, 18458–18462.

[13] W. Zhou, T. Jia, H. Shi, D. Yu, W. Hong, X. Chen, *J. Mater. Chem. A* **2019**, *7*, 303–311.

[14] M. Sachs, R. S. Sprick, D. Pearce, S. A. J. Hillman, A. Monti, A. A. Y. Guilbert, N. J. Brownbill, S. Dimitrov, X. Shi, F. Blanc, et al., *Nat. Commun.* **2018**, *9*, 1–11.

[15] L. Guo, Y. Niu, S. Razzaque, tan, S. Jin, *ACS Catal.* **2019**, *9*, 9438–9445.